CMS Hadronic Endcap Calorimeter Upgrade Studies for SLHC "P-Terphenyl Deposited Quartz Plate Calorimeter Prototype"

Ugur Akgun, Elif A. Albayrak, Gural Aydin, Burak Bilki, Peter Bruecken, Kerem Cankocak, Warren Clarida, Lucien Cremaldi, Firdevs Duru, Anthony Moeller, Alexi Mestvirishvili, Yasar Onel, Ferhat Ozok, Justin Parsons, David Sanders, Nasuf Sonmez, James Wetzel, David Winn, and Taylan Yetkin

***Abstract*—The Large Hadron Collider (LHC) is going to start taking data with $10^{33}\ \mathrm{cm^{-2}s^{-1}}$ luminosity, and reach the designed value of $10^{34}\ \mathrm{cm^{-2}s^{-1}}$ in 2013. The LHC luminosity will continue to improve each year, reaching to $10^{35}\ \mathrm{cm^{-2}s^{-1}}$ in 2023. We call this high luminosity era the Super-LHC (SLHC). Hadronic Endcap (HE) calorimeters of the CMS experiment cover the pseudorapidity range of $1.4 < \eta < 3$ on both sides of the CMS detector, contributing to superior jet and missing transverse energy resolutions. As the integrated luminosity of the LHC increases, the scintillator tiles used in the CMS Hadronic Endcap calorimeter will lose their efficiency.**

The CMS collaboration plans to substitute Quartz plates for the scintillator tiles of the original design. Various tests have proved Quartz to be radiation hard, but the light produced by Quartz comes from Cerenkov process, which yields drastically fewer photons than scintillation. To increase the light collection efficiency, we propose to treat the Quartz plates with radiation hard wavelength shifters, p-terphenyl or 4% gallium doped zinc oxide. The test beam studies revealed a substantial light collection increase on pTp or ZnO:Ga deposited Quartz plates. We constructed a 20 layer calorimeter prototype with pTp coated plates, and tested the hadronic and the electromagnetic capabilities at the CERN H2 area. Here we report the results of these test beams as well as radiation damage studies performed on p-Terphenyl.

***Index Terms*—Calorimeter, p-terphenyl, Quartz, radiation damage, zinc oxide.**

I. Introduction

THE Large Hadron Collider (LHC) is designed to provide a 14 TeV center of mass energy with p-p collisions every 25 ns. The starting peak luminosity of the accelerator is going to be $10^{33}\ \mathrm{cm^{-2}s^{-1}}$. This value is planned to increase each year, reaching $10^{34}\ \mathrm{cm^{-2}s^{-1}}$ in 2013. In the current design, the luminosity is limited by beam dumping, machine collimation and protection systems, as well as electron cloud effects. There are two possible luminosity upgrade paths; early separation and Large Piwinski angle scenarios. The early separation scenario proposes installation of early separation dipoles at about 3 m from the interaction points of the ATLAS and CMS detectors. In the Large Piwinski angle scenario, the bunch spacing is doubled and bunches are proposed to be longer, more flatter and more intense [1], [2].

Current luminosity upgrade plans are divided into two 5-year phases. Phase 1 covers the period from 2013 to 2018 when the peak luminosity will increase from $10^{34}\ \mathrm{cm^{-2}s^{-1}}$ to $4 \times 10^{34}\ \mathrm{cm^{-2}s^{-1}}$. Phase 2 covers from 2018 to 2023 when the peak luminosity reaches $10^{35}\ \mathrm{cm^{-2}s^{-1}}$.

If, as widely predicted, the LHC discovers the Higgs boson, the accumulated luminosity will only be enough to study mass and few branching ratios, but not to measure more challenging topics like Higgs self couplings. The SLHC will provide high statistics to study rare events: massive MSSM Higgs, Higgs couplings to itself, to bosons and fermions, and new physics signatures such as supersymmetry and massive neutrinos.

The accelerator luminosity upgrade will require detectors to be modified for higher radiation conditions as well. The Hadronic Endcap (HE) calorimeter of the Compact Muon Solenoid (CMS) experiment is one of these detectors. In the current design, the CMS HE calorimeter consists of 19 layers of scintillator tiles sandwiched between 70 mm brass absorbers. Light generated in these scintillators (Kuraray SCSN81) is carried to hybrid photodiodes by Kuraray Y-11 double clad wavelength shifting (WLS) fibers. Both scintillators and WLS fibers have been shown to be moderately radiation hard up to 25 kGy [3]. The simulation studies show that the expected radiation levels have strong η dependency [4], [5]. Fluka and Geant simulations, which are performed assuming 10 years of LHC runs at $10^{34}\ \mathrm{cm^{-2}s^{-1}}$ luminosity, predict radiation levels up to 100 kGy in high η towers. This value reaches up to 300 kGy for the front towers of the $2.9 < \eta < 3.0$ region, where the Endcap Electromagnetic (EE) calorimeter does not shield the HE calorimeter.

With the increasing luminosity plan for LHC, we expect the scintillator tiles and plastic WLS fibers to face higher radiation levels than these reports. Hence, the resolution of the HE calorimeter will deteriorate faster, starting from high η towers. As a solution to this radiation damage problem, we propose to

Manuscript received September 13, 2009; revised November 17, 2009. Current version published April 14, 2010.This work was supported by the U.S. Department of Energy (DE-FG02-91ER-40664).

U. Akgun, E. A. Albayrak, G. Aydin, B. Bilki, P. Bruecken, K. Cankocak, W. Clarida, F. Duru, A. Moeller, A. Mestvirishvili, Y. Onel, F. Ozok, J. Parsons, J. Wetzel, and T. Yetkin are with the University of Iowa, Iowa City, IA 52242 USA (e-mail: ugur-akgun@uiowa.edu).

L. Cremaldi is with the University of Mississippi, University, MS 38677 USA.

D. Sanders is with the Physics and Astronomy Department, University of Mississippi, University, MS 38677 USA.

N. Sonmez is with Ege University, 35040 Bornova-Izmir, Turkey.

D. Winn is with Fairfield University, Fairfield, CT 06430 USA.

Color versions of one or more of the figures in this paper are available online at http://ieeexplore.ieee.org.

Digital Object Identifier 10.1109/TNS.2010.2040038

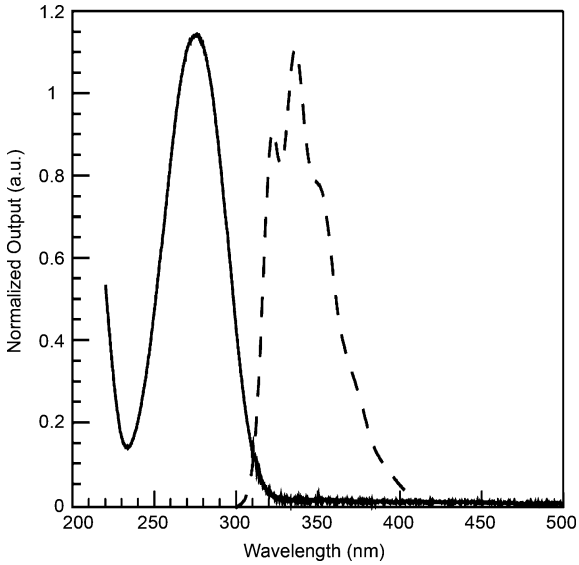

Fig. 1. Absorption (solid line) and emission (dashed line) spectra of p-Terphenyl.

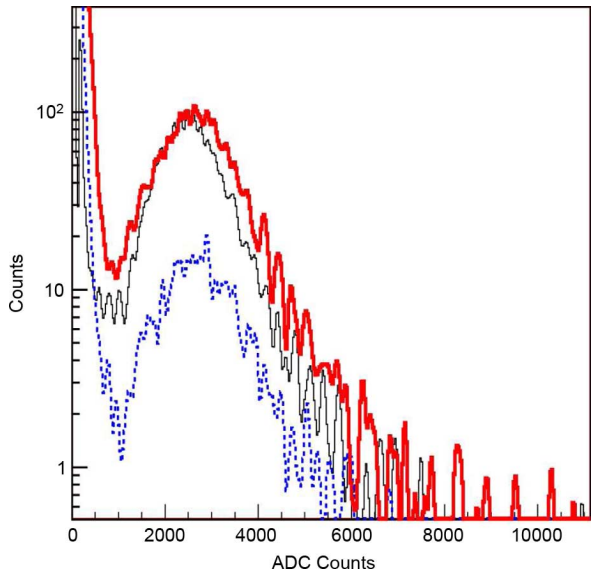

Fig. 2. The comparison of single photoelectron level signal distributions from 2 μm thickness of pTp (thick solid line), and 0.2 μm of ZnO:Ga (thin solid line) deposited plates to that of a plain Quartz plate (thick dashed line).

substitute Quartz plates for the scintillator tiles. In previous papers, we reported results from radiation hardness tests on various types of Quartz material in the form of fiber under electron, proton, neutron, and gamma irradiations. Results show that Quartz can withstand the radiation doses of up to 12.5 MGy [6]–[8].

However, with the Quartz plates, the detected photons come from Cerenkov radiation, which yields 100 times less light than the scintillation process in visible region [9], [10]. On the other hand, the number of created Cerenkov photons increases with $1/\lambda^2$ (λ being the wavelength). This gives us the opportunity to collect more photons by using wavelength shifters with absorption spectra (see Fig. 1) positioned in UV range. Then again, the interaction of particles with the scintillating layer also increases the total number of counts. For this purpose, we tested different wavelength shifters including p-terphenyl (pTp) [11], 4% gallium dopped zinc oxide (ZnO:Ga), o-terphenyl (oTp), m-terphenyl (mTp) and p-quarterphenyl (pQp).

The wavelength shifter deposited on the Quartz has to be radiation hard as well. We tested the most feasible candidate, pTp, for proton irradiation up to 400 kGy. in the Indiana University Cyclotron Facility (IUCF) and CERN beam lines.

Eventually, we constructed a 20 layer sampling calorimeter prototype with pTp deposited Quartz plates as active medium. We tested this calorimeter's hadronic and electromagnetic capabilities at the CERN H2 area. This note summarizes the results from the tests described above.

II. Selection of Wavelength Shifter

To improve the light production inside the Quartz plates, we considered various wavelength shifters as coatings: pTp, ZnO:Ga, oTp, mTp, and pQp. Other than ZnO:Ga, all of them can be evaporated in a vacuum chamber to be applied on Quartz. The molecular properties of ZnO:Ga do not allow evaporation, so RF sputtering was used for this case. We have prepared Quartz plates with various wavelength shifters deposited at different thicknesses at the University of Iowa CMS laboratories and Fermilab Thin Film Laboratory. The light readout was performed from the edge of each plate with Hamamatsu R7525-HA photomultiplier tubes (PMTs) [12]–[14].

Standalone units, with single Quartz plate and a single PMT, were prepared to test various wavelength shifting materials and thicknesses. The beam tests at the Fermilab Meson Test Beam Facility and at the CERN H2 area, showed that the one sided coatings with 2 μm thickness of pTp and 0.2 μm of ZnO:Ga yield the best results with pion, proton, and electron beams of various energies. Fig. 2 shows the comparison of single photoelectron level signal distributions from 2 μm thickness of pTp and 0.2 μm of ZnO:Ga deposited plates to that of a plain Quartz plate. All three plates were placed to same shower depth during the same run of 50,000 triggers, and each PMT gain were set to 10^6. Using pTp or ZnO:Ga, we have increased the probability of seeing a photon by at least a factor of four compared to plain Quartz plates. Since ZnO:Ga requires a more expensive and delicate deposition process, we decided to focus on pTp for the rest of our studies.

The radiation hardness of pTp was tested, with proton beams, at the Indiana University Cyclotron Facility (IUCF) and CERN beam lines. The ^{90}Sr activated scintillation light outputs of pTp samples both before and after irradiation were compared in the University of Mississippi CMS Laboratories. We also employed the liquid scintillation technique in which the pTp samples were mixed in a saturated toluene solution with a standard tritium beta source and scintillation light was analyzed for dosed and standard samples. The toluene yields negligible scintillation light in the tests. The dosed pTp samples were also sent for chemical analysis showing slight breakdown of the tri-ring pTp molecule into simpler benzene ring forms. The results of different irradiation levels are reported in Fig. 3. After 200 kGy of proton irradiation, the light output drops to 84% of the initial level. But the initial radiation damage rate slowly flattens, and after 400 kGy

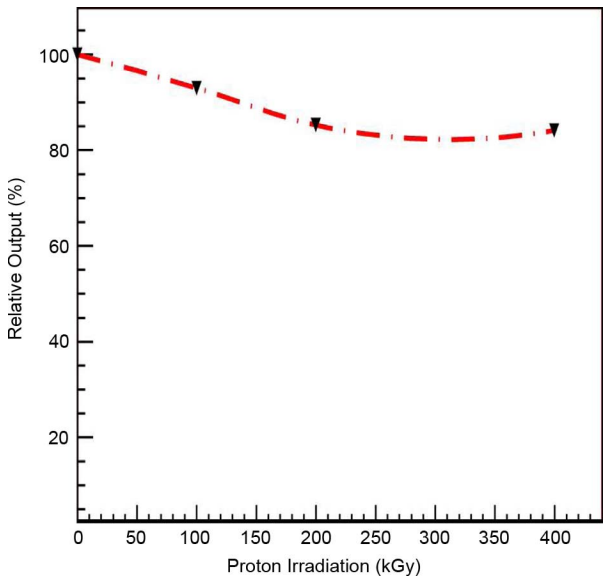

Fig. 3. Light output from pTp sample after proton irradiation versus proton irradiation level with simple fitted line.

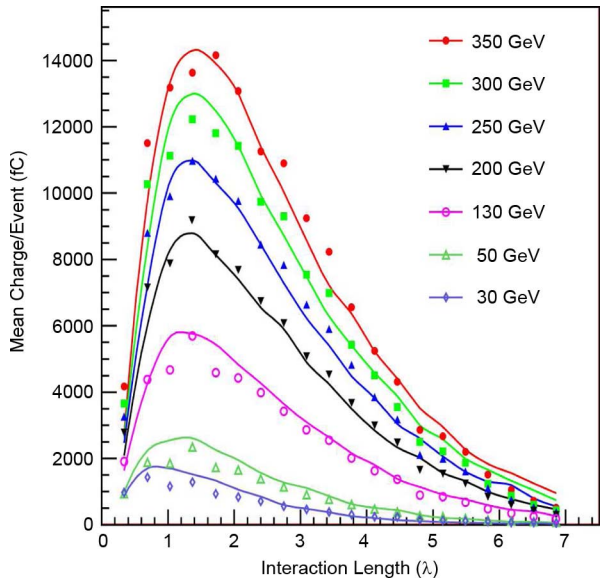

Fig. 4. Longitudinal shower profile for various π^- beam energies. Along with data points, simulation results are also shown with solid lines.

of radiation we still observed less than a 20% loss of light production.

III. pTp Deposited Quartz Plate Calorimeter Prototype

A. The Design and Test Setup

In light of the studies described in the previous section, we have built a Quartz plate calorimeter prototype with $0.2\ \mu\mathrm{m}$ pTp deposited on one side of the Quartz tiles. The prototype consists of 20 layers of Quartz plates $(15\ \mathrm{cm} \times 15\ \mathrm{cm} \times 5\ \mathrm{mm})$ with 7 cm iron absorbers between each layer. Since the CMS HE calorimeter has 19 layers of 7 cm brass absorbers, our prototype model is a very good representation of the small solid angle of the upgraded HE calorimeter. GE-124 Quartz from GE Quartz Company was used as the material for the plates. After $2\ \mu\mathrm{m}$ pTp was deposited on every Quartz plate via evaporation at Fermilab Thin Film Laboratory, one inch section on the side of each plate was polished at the University of Iowa CMS Laboratories for better PMT coupling. The light generated in the Quartz plate was read out by Hamamatsu R7525-HA PMTs from the polished region.

The Quartz plates were wrapped with aluminized mylar for good reflectivity, especially in the UV range, and then with Dupont Tyvek for a robust light tight structure. Every Quartz plate and PMT system was prepared to be a standalone unit. Having our prototype constructed as a collection of standalone units allowed us to change the absorber thickness between layers for a possible electromagnetic configuration.

The prototype was tested at the CERN H2 test area with two different configurations: a hadronic configuration with 7 cm iron absorbers between each layer, and an electromagnetic (EM) configuration with 2 cm iron absorbers. In the hadronic configuration, π^- beams with 30, 50, 80, 130, 200, 250, 300, and 350 GeV energies were used. In the EM configuration electron beams with energies of 50, 80, 100, 120, 150 and 175 GeV were utilized.

The readout was performed by charge integration and encoding units [15], [16] and the data was stored in CMS SoftWare HCAL Test Beam raw data format [17]. Each QIE channel was readout in 20 time slices of 25 ns length each. The trigger was given by the coincidence of four scintillation counters of sizes $14\ \mathrm{cm} \times 14\ \mathrm{cm}$ and $4\ \mathrm{cm} \times 4\ \mathrm{cm}$ and $2\ \mathrm{cm} \times 2\ \mathrm{cm}$. Therefore, a beam spot of size $2\ \mathrm{cm} \times 2\ \mathrm{cm}$ is anticipated. A downstream muon veto counter in the beamline was used to exclude the muon contamination in the beam from analysis.

B. The Hadronic and Electromagnetic Capabilities of the Prototype

The response read out from each PMT was normalized to the gain of the PMT reading out the first plate. The total calorimeter response was then reconstructed by adding the individual responses from all chambers.

The calorimeter prototype was simulated using GEANT4 [18], [19], LHEP physics package. The pTp scintillation properties were sampled from Fig. 1. The model consisted of an identical setup in terms of geometry and the materials involved other than the PMTs for which the response was simulated as the total number of photons that reach the PMT window location with a wavelength within the acceptance range of the PMT. 80 GeV π^- beam data was used to calibrate the simulation results. So, the simulation of 80 GeV π^- beam was excluded from the analysis not to bias the overall results). Fig. 4 shows the longitudinal shower profile for different energies. Solid lines represent the simulation results for corresponding energies and are simple curves connecting the simulation output points. Data and simulation results are consistent within statistical fluctuations. Fig. 5 shows the charge distribution of the calorimeter prototype with 300 GeV π^- beam at hadronic configuration.

Fig. 6 shows the detector linearity for the test of the prototype in hadronic calorimeter setup with various π^- beam energies. Data (simulation) points are indicated with hollow circles

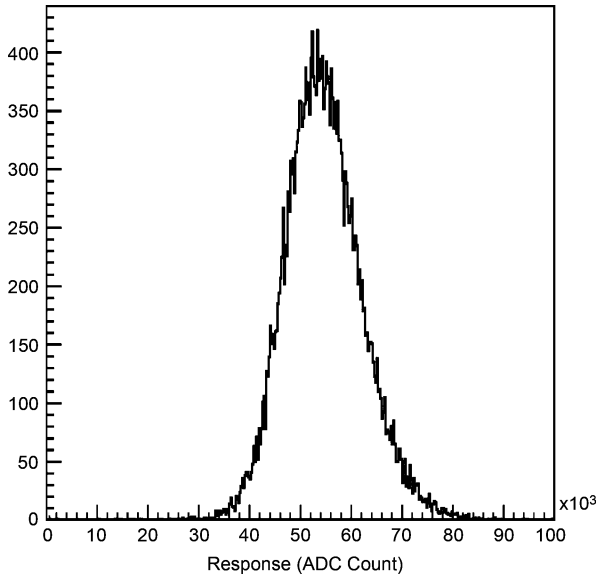

Fig. 5. 300 GeV pion response of the calorimeter prototype on hadronic configuration.

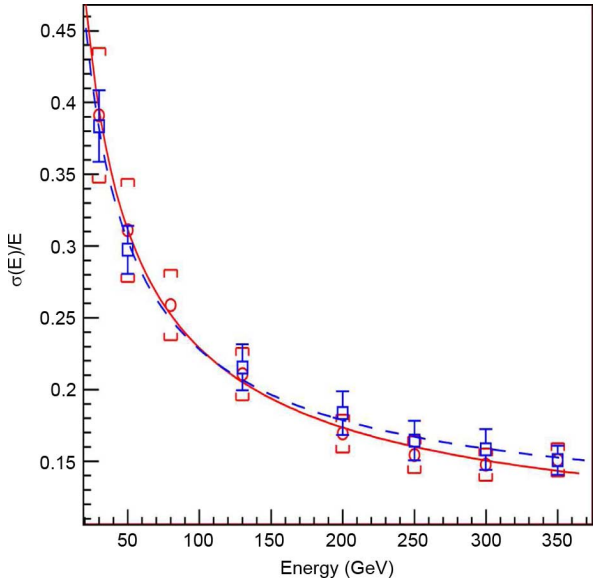

Fig. 7. Hadronic energy resolution, data (circle-solid line) and Geant4 simulations (square-dashed line), for the calorimeter prototype.

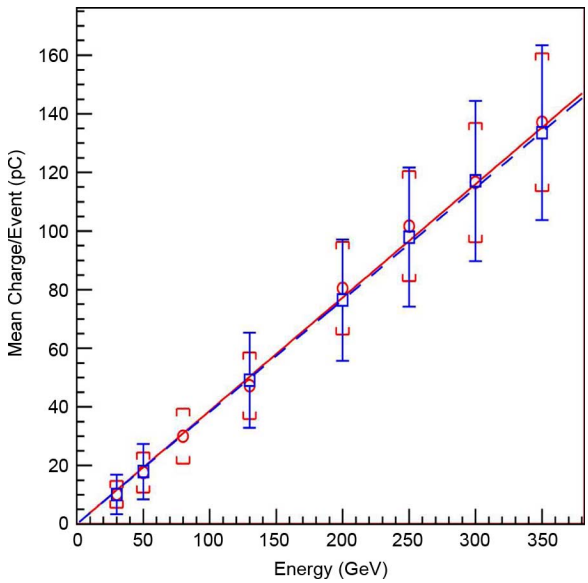

Fig. 6. Detector linearity graph, data (circle-solid line) and Geant4 simulations (square-dashed line), for the hadronic calorimeter prototype. Lines are fits to a first order linear dependence.

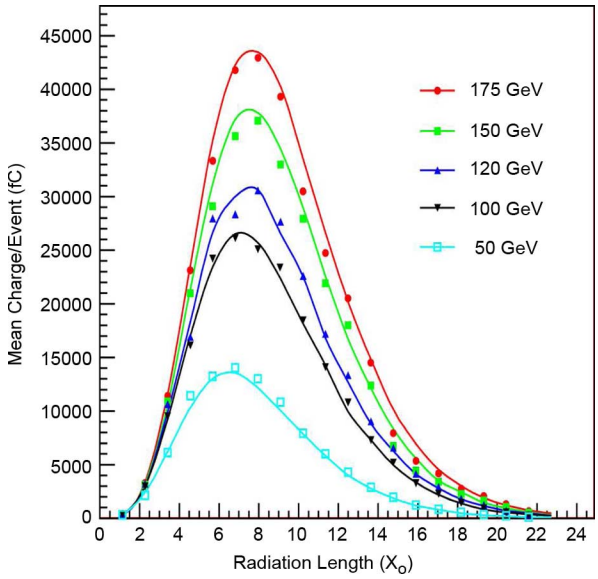

Fig. 8. Longitudinal shower profile for various electron beam energies. Along with data points, simulation results are also shown with solid lines.

(squares). Solid lines are the fits to the data and simulation points which yield around 1% hadronic response linearity. Both data and the simulation exhibit similar linear beahavior. The larger deviations of the data points from the fit is due to limited statistics compared to the simulation results.

Fig. 7 shows the energy resolution of the hadronic calorimeter together with the prediction of the simulations. Both data and simulation results are fitted to the non-compensated energy resolution parametrized as;

$$\frac{\sigma(E)}{E} = \frac{A}{\sqrt{E}} \oplus \frac{B}{E} \oplus C \qquad (1)$$

where A is the stochastic term, B is the noise term and C is the constant term (they are indicated as p0, p1 and p2 as the fit parameters in the figure). Data and simulation results have similar behavior with a negligible noise term and a constant term under 10%. Overall, the hadronic energy resolution can be expressed as;

$$\frac{\sigma(E)}{E} = \frac{210.3\%}{\sqrt{E}} \oplus 8.8\%. \qquad (2)$$

Although the purpose of these studies is to find a solution for radiation hardness problems of the CMS HE calorimeter, we took this opportunity to test the similar radiation hard configuration on an electromagnetic calorimeter. The total calorimeter response was reconstructed by adding the individual layer

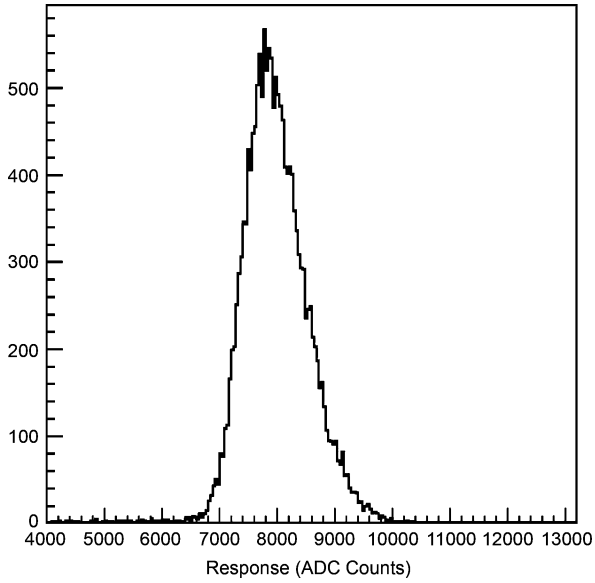

Fig. 9. 100 GeV electron response of calorimeter prototype with electromagnetic configuration.

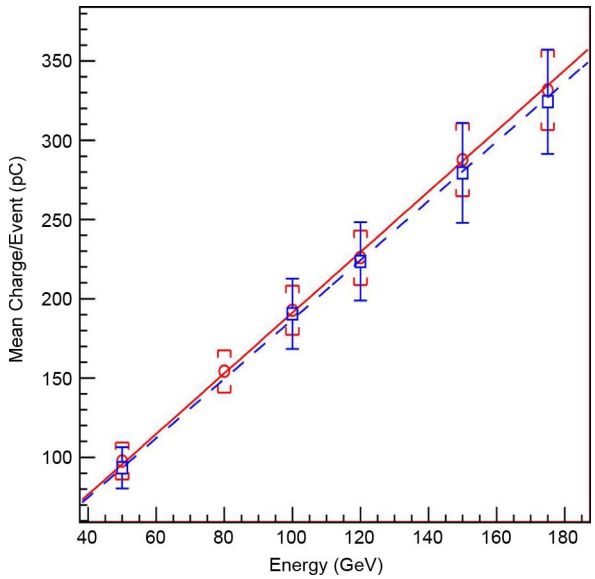

Fig. 10. Detector linearity, data (circle-solid line) and Geant4 simulations (square-dashed line), for the electromagnetic calorimeter prototype. Solid lines are fits to a first order linear dependence.

responses after gain normalizations and pedestal subtractions same as for the hadronic calorimeter case. The readout was identical with the hadronic setup. A seperate calibration for the simulations at 80 GeV electron incidence was performed since the calorimeter has a compensation factor different than unity (the E_π/E_e ratio was measured as 0.88 at 80 GeV). Therefore, the simulations with 80 GeV electron beam are excluded from the analysis. Fig. 8 shows the longitudinal shower profile for different electron beam energies. Shower development is well predicted by the simulations. Fig. 9 shows the charge distribution of the calorimeter with 100 GeV electron beam.

Fig. 10 shows the detector linearity for the prototype in electromagnetic calorimeter setup to be within 3%. The linearity

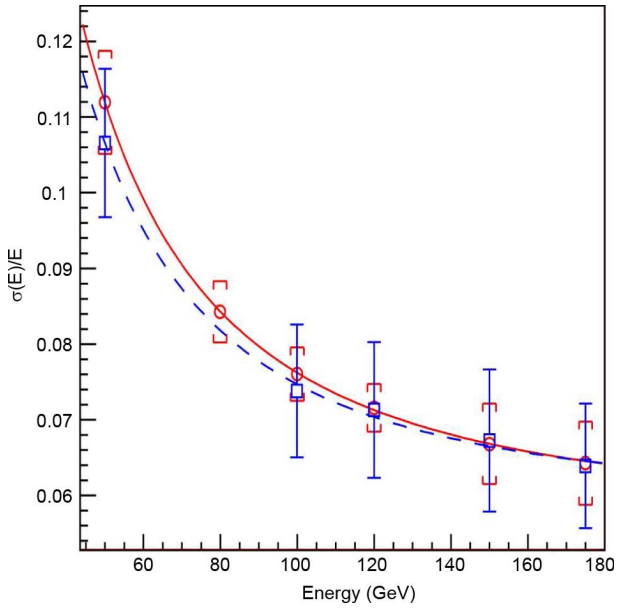

Fig. 11. Electromagnetic energy resolution, data (circle-solid line) and Geant4 simulations (square-dashed line), for the calorimeter prototype.

factor is well predicted by the simulations within a few standard deviations. The energy dependence of the electromagnetic response linearity is much stronger than that of the hadronic calorimeter. The linear behavior of the detector is satisfactory for calibration and operation purposes.

Fig. 11 shows the electromagnetic energy resolution. The solid lines are the fits to the energy resolution parametrized in the hadronic calorimeter section. The simulation predicts better resolution for lower values of beam energy. For energies greater than 120 GeV, both resolution curves converge to a constant value of around 5.6%. The overall energy resolution of the electromanetic calorimeter is calculated as;

$$\frac{\sigma(E)}{E} = \frac{26\%}{\sqrt{E}} \oplus \frac{4.5\%}{E} \oplus 5.6\%. \tag{3}$$

IV. Conclusion

As the peak luminosity of the LHC increases, detector upgrades are required for LHC experiments. The CMS experiment HE calorimeter consists of moderately radiation hard scintillator tiles, and they are not going to survive the high radiation environment of the SLHC. This report shows that pTp deposited Quartz plates are a perfect candidate to replace the scintillator tiles of the CMS HE calorimeter. Both Quartz and pTp are radiation hard and cost effective options.

We have demonstrated that with 2 μm pTp coatings on one side and 0.2 μm ZnO:Ga (4% gallium doped zinc oxide), the light production can be enhanced by at least a factor of 4. We also report that pTp loses only 16% of the light production after 400 kGy proton irradiation. This is well above the predicted SLHC radiation levels for most of the HE towers.

To test the calorimeter capabilities of this replacement option, we constructed a 20 layer pTp deposited Quartz plate calorimeter prototype. The test beam results show that the

prototype with a $15\ \mathrm{cm} \times 15\ \mathrm{cm}$ active area yields around 15% hadronic energy resolution for 350 GeV π^- beam. Even with the considerable energy leakage from the undersize prototype, this is a very promising result. On a larger scale, pTp deposited Quartz plate calorimeter is promising in terms of achieving the current HE calorimeter performance, which is around 8% in hadronic energy resolution at a 300 GeV pion beam energy.

Although it is out of the scope of this study, we reconfigured the prototype as an electromagnetic calorimeter and tested it at various electron beam energies. We got very encouraging results, suggesting that pTp deposited Quartz plates sandwiched between thinner absorbers can be used as a highly radiation hard EM calorimeter option for future collider experiments. Considering the radiation damage issues of the CMS Endcap Electromagnetic calorimeter, we propose that pTp deposited Quartz plates should be used in all CMS endcap regions. This includes the EM section where 2 cm absorbers should be used, and the hadronic section where 7 cm brass absorbers already are in use.

ACKNOWLEDGMENT

The authors would like to thank CERN H2, and Fermilab Meson beam test, and Indiana University Cyclotron facilities. The authors especially would like to thank Eileen Hahn from Fermilab Thin Film laboratory for her amazing efforts on pTp, and ZnO:Ga depositions. The authors are indebted to our CMS HCAL Collaborators D. Green, J. Freeman, and A. Skuja for their support and encouragement, the QUARKNET students for their help during the construction of the prototypes. The authors would also like to thank the University of Iowa Office of Vice-President of Research, for its support.

REFERENCES

[1] S. Abdullin *et al.*, Physics Potential and Experimental Challenges of the LHC Luminosity Upgrade, hep-ph/0204087, 2002.

[2] W. Scandale and F. Zimmermann, "Scenarios for sLHC and vLHC," *Nucl. Phys. B (Proc. Suppl.)*, pp. 207–211, 2008.

[3] The HCAL Tech. Design Rep., CERN/LHCC 97-31, CMS TDR 2 1997.

[4] M. Huhtinen, "The Radiation Environment at the CMS Experiment at the LHC," Ph.D dissertation, Helsinki Univ. of Technology, Helsinki, Finland, 1996.

[5] I. Golutvin *et al.*, Simulation of Radiation Damage in HE Scintillating Tiles and Pion Energy Resolution After 10 Years of LHC Operation, CMS-Note 2002/013.

[6] I. Dumanoglu *et al.*, "Radiation-hardness studies of high-OH content Quartz fibres irradiated with 500 MeV electrons," *Nucl. Instrum. Methods Phys. Res. A*, vol. A490, pp. 444–455, 2002, CMS-Note 2001/020.

[7] K. C. Cankocak *et al.*, "Radiation-hardness measurements of high-OH content fibers irradiated with 24 GeV protons up to 1.25 Grad," *Nucl. Instrum. Methods Phys. Res. A*, vol. A585, pp. 20–27, 2008.

[8] U. Akgun and Y. Onel, "Radiation-hard Quartz Cerenkov calorimeters," in *Proc. Amer. Institute of Physices Conf.*, 2006, vol. 867, pp. 282–289.

[9] U. Akgun *et al.*, "Quartz plate calorimeter as SLHC upgrade to CMS hadronic endcap calorimeters," in *Proc. 13th Int. Conf. Calorimetry in High Energy Physics*, Pavio, Italy, 2008.

[10] F. Duru *et al.*, "CMS hadronic endcap calorimeter upgrade studies for SLHC—Cerenkov light collection from Quartz plates," *IEEE Trans. Nucl. Sci.*, vol. 55, no. 2, pp. 734–740, Apr. 2008.

[11] D. Bartlett *et al.*, "Performance of the Cherenkov counters in the fermilab tagged photon spectrometer facility," *Nucl. Instrum. Methods Phys. Res. A*, vol. A260, pp. 55–75, 1987.

[12] U. Akgun *et al.*, "Comparison of PMTS from three different manufacturers for the CMS-HF forward calorimeter," *IEEE Trans. Nucl. Sci.*, vol. 51, no. 4, pp. 1909–1915, Aug. 2004.

[13] U. Akgun *et al.*, "Complete tests of 2000 Hamamatsu R7525HA phototubes for the CMS-HF forward calorimeter," *Nucl. Instrum. Methods Phys. Res. A*, vol. A550, pp. 145–156, 2005, CMS-NOTE-2004-019.

[14] U. Akgun *et al.*, "Afterpulse timing and rate investigation of three different Hamamatsu photomultipler tubes," *J. Instrum.*, 2008, 3 T01001.

[15] T. Zimmerman *et al.*, "The SVX2 readout chip," *IEEE Trans. Nucl. Sci.*, vol. 42, no. 4, pp. 803–807, Aug. 1995.

[16] T. Zimmerman and J. R. Hoff, "The design of a charge-integrating modified floating-point ADC chip," *IEEE J. Solid State Circuits*, vol. 39, pp. 895–895, 2004.

[17] [Online]. Available: https://twiki.cern.ch/twiki/bin/view/CMS/WorkBookCMSSWFramework

[18] S. Agostinelli *et al.*, "Geant4—A simualtion toolkit," *Nucl. Instrum. Methods Phys. Res. A*, vol. A506, pp. 250–303, 2003.

[19] J. Allison *et al.*, "Geant4 developments and applications," *IEEE Trans. Nucl. Sci.*, vol. 53, no. 1, pp. 270–278, Feb. 2006.